J Mater Sci: Mater Electron **(2025) 36:3**

DLTS characterisation of 107 MeV krypton ion-irradiated nitrogen-doped 4*H*-silicon carbide

Ezekiel Omotoso[1,2,*], Emmanuel Igumbor[3], and Walter E. Meyer[2]

[1] *Department of Physics and Engineering Physics, Obafemi Awolowo University, Ile-Ife 220005, Nigeria*
[2] *Department of Physics, University of Pretoria, Pretoria 0083, South Africa*
[3] *Department of Mechanical Engineering Science, University of Johannesburg, Johannesburg, South Africa*

Received: 4 July 2024
Accepted: 8 December 2024
Published online: 18 December 2024

ABSTRACT

Swift heavy ions, such as krypton ions, play a significant role in developing and enhancing the performance of various devices. In this study, the influence of Kr^{2+} on nitrogen-doped 4*H*-silicon carbide has been investigated using deep level transient spectroscopy (DLTS). Krypton ions, with an energy of 107 MeV, were used to irradiate the Au/Ni/4*H*-SiC Schottky barrier diodes (SBDs) at a fluence of 1×10^{10} cm^{-2} at room temperature (300 K). Before the irradiation of the samples, the electrical measurements revealed good rectifying behaviour. However, rectification properties of the Au/Ni/4H-SiC SBDs were completely lost after irradiation at a fluence of 1×10^{10} cm^{-2}. Annealing was performed at 300 °C in flowing argon, and the current–voltage (I–V) and capacitance–voltage (C–V) revealed partial rectification. DLTS of the as-grown devices analyses revealed the presence of four deep level defects. After annealing the irradiated device, the DLTS spectra showed a reduction in the intensity of the $E_{0.10}$ and the disappearance of the $E_{0.12}$ as well as the $E_{0.16}$ defects compared to that as-grown. Two defects with energies of 280 and 410 meV showed inverted peaks, as would have been expected from minority carriers trap instead of majority carriers, which led to confusion as the peaks were inverted. It was concluded that the peculiar characteristics of DLTS measurements on SBDs may be due to the extremely high value of the series resistance as well as the low capacitance. The results of this study provide insight into the behaviour of SBDs under extreme irradiation and can be used to improve the radiation tolerance of electronic devices made from SiC.

1 Introduction

Schottky barrier diodes (SBDs) are a type of semiconductor diode that is characterized by the formation of a Schottky barrier at the metal–semiconductor interface [1]. The Schottky barrier, which occurs due to the difference between the work function of the metal and the semiconductor, is responsible for the unique electrical properties of SBDs, such as their fast-switching speeds and low forward voltage drop, V_f (the voltage required for diode to conduct current in the forward direction) [2]. SBDs have been widely studied and used in many electronic devices, such as power electronics, high-frequency switching,

Address correspondence to E-mail: omotoeze@gmail.com; eomotoso@oauife.edu.ng

https://doi.org/10.1007/s10854-024-14060-8

and sensing applications [3, 4]. They are particularly attractive in high-frequency and high-temperature applications because of their low reverse leakage current and low capacitance compared to other wide bandgap semiconductors [5]. One of the critical factors in the performance of SBDs is the high quality of the metal–semiconductor interface, i.e., the Au/Ni/4H-silicon carbide (SiC) interface [6]. Studies have shown that the Schottky barrier height (SBH) is directly related to the quality of the interface, with a lower SBH resulting in a lower forward voltage drop and a lower reverse breakdown voltage [7, 8]. Many researchers have employed different techniques to improve the quality of the interface, such as thermal annealing (as in the case of Ni ohmic contacts on 4H– 4H–SiC), sputtering, and chemical vapour deposition (CVD) [9–12]. Also, the performance of the SBDs is influenced by the level of doping of the semiconductor or irradiation of the device by energetic particles (e.g., krypton ions). It has been reported that increasing the doping level in 4H–SiC results in a higher SBH and a lower reverse breakdown voltage [13]. Furthermore, an extremely high doping level in a semiconductor brings about an increase in the reverse leakage current as well as a reduction in forward current [14]. SBDs based on nitrogen-doped 4H–SiC have also been extensively studied in the recent years due to their high thermal stability and high electron mobility. This semiconductor material, 4H–SiC, has shown great potential for high-temperature and high-power electronics device applications [11, 15].

SiC is a wide bandgap semiconductor material with many applications in high-power, high-temperature, and high-frequency electronic devices due to its high thermal stability and electron mobility [4, 16]. It crystallises in multiple polytypes depending on the growth conditions. One of the most used polytypes is 4H–SiC, which has a hexagonal crystal structure and lattice constant of about 3.085 Å [17, 18]. The 4H polytype has a high electron mobility, thermal conductivity, and breakdown electric field [19]. However, as in most semiconductor materials, 4H-SiC is not without defects [20]. It can contain defects that can impact its optical and electronic properties. Some of these deep level defects can be introduced purposefully. For instance, impurity doping of 4H–SiC with nitrogen has been used to reduce the resistivity of devices [21]. In another, particle irradiation has been used to reduce the lifetime of carriers in 4H–SiC-related devices, thereby increasing the switching speeds [9, 22–27].

Furthermore, different defects have been unintentionally introduced into 4H–SiC via crystal growth [9, 22–27]. The most commonly studied defects in nitrogen-doped 4H-SiC include point defects, extended defects, and defect complexes [28–30]. Point defects such as silicon or carbon vacancies and carbon interstitials in nitrogen-doped 4H–SiC have been reported [25, 31]. Silicon or carbon vacancies are defects where a silicon or carbon atom is removed from the normal lattice site [32]. In contrast, carbon interstitial is a defect where a carbon atom is present in an extra lattice position [25, 31]. Point defects in 4H–SiC can also be classified as intrinsic defects, such as vacancies and interstitials, and extrinsic defects, such as impurities and structural defects. These defects can have a significant influence on the electrical and optical properties of 4H–SiC, such as its carrier mobility, bandgap, and threshold voltage of Field-Effect Transistors (FETs) made on the material [33]. Since these defects can either be beneficial or harmful to the application of SBDs, understanding and controlling them is crucial for the development of high-performance 4H–SiC devices. In general, various techniques, such as transmission electron microscopy (TEM), scanning electron microscopy (SEM), secondary ion mass spectroscopy (SIMS), Raman spectroscopy, X-ray diffraction (XRD) and deep level transient spectroscopy (DLTS), have been employed to study, detect, and characterize defects in nitrogen-doped 4H–SiC [15, 34–36]. Therefore, the knowledge of these defects are important for understanding and improving the performance of 4H–SiC-based electronic devices for electronic, industrial and laboratory applications.

DLTS is a powerful and well-established technique for characterizing defects in semiconductor materials (such as 4H–SiC) [15]. The technique has been widely used and reported to characterize defects present in unirradiated as well as irradiated semiconductor devices [9, 23–25, 37]. DLTS has been used to study the influence of swift heavy ion irradiation (such as Kr^{2+}) on nitrogen-doped 4H-SiC, a widely used semiconductor for high-temperature and high-power electronics. Kalinina et al. have reported the effect of 245 MeV Kr^{2+} irradiation at a fluence of 10^{10} ions.cm^{-2} on the electrical properties of Cr/4H-SiC Schottky barrier diodes with an epitaxial layer of donor concentration of 4–5 × 10^{15} cm^{-3} [27]. DLTS was employed by Kalinina et al. to characterize the deep levels present

and discovered an increase in the concentration of the *Z1* defect observed in irradiated samples [27]. Photoluminescence and DLTS have been used to study the influence of irradiation on the optical and electrical properties of the nitrogen-doped 4H-SiC epitaxial layer. The concentration of the uncompensated donor of the nitrogen-doped 4H-SiC epitaxial layer is 5–8 × 10^{15} cm^{-3} with the help of fast neutrons, 245 MeV Kr^{2+} and 710 MeV Bi^{2+} irradiation [38]. According to *ref.* [38], the 245 MeV Kr^{2+} and 710 MeV Bi^{2+} induce defects with the same parameters as those of electrons, neutrons, and light ions. Another study by Kalinina et al. also reported that capacitance- (C–), current- (*I*–) and charge- (*Q*–) DLTS discovered the presence of the well-known *Z1* defect with activation energy 0.66 eV after bombarding the CVD-grown 4H–SiC of the epitaxial layer of donor concentration of 4–5 × 10^{15} cm^{-3} with 245 MeV Kr^{2+} to a fluence of 10^{10} ions.cm^{-2} [39]. Broniatowski et al. reported the peculiar features obtained when characterized resistive samples with the DLTS [40]. The peculiarity characteristics brought about a reduction in the DLTS signal or even reversed its sign, which leads to potential confusion between the minority and majority carrier traps. This characteristic was demonstrated using ion-implanted silicon and germanium bicrystal. However, the influence of 107 MeV Kr^{2+} at a fluence of 1.0 × 10^{10} cm^{-2} on the electrical properties of Au/Ni/nitrogen-doped 4H–SiC SBDs with low donor concentration of 4.0 × 10^{14} cm^{-3} in the epitaxial layer has not been reported. Additionally, information on the behaviour of DLTS signals observed during the characterisation of highly resistive Au/Ni/nitrogen-doped 4H–SiC SBDs has not been reported.

The purpose of investigating the electrical properties of Au/Ni/nitrogen-doped 4H–SiC SBDs after 107 MeV Kr^{2+} irradiation at a fluence of 1.0 × 10^{10} cm^{-2} is to simulate the irradiation conditions that devices may encounter in space applications. This low doping density material and irradiation fluence stand for the environment that space-based electronic devices fabricated using 4H–SiC would experience. Therefore, understanding the impact of this specific irradiation on the electrical properties of Au/Ni/nitrogen-doped 4H–SiC SBDs, as well as the DLTS behaviour in these highly resistive devices, is important for improving the radiation tolerance of electronic devices made from 4H–SiC.

In this study, DLTS is used to investigate the effects of 107 MeV Kr^{2+} on Au/Ni/nitrogen-doped 4H–SiC devices at a fluence of 1.0 × 10^{10} cm^{-2}. The irradiation on this low doping density semiconductor (Au/Ni/nitrogen-doped 4H-SiC) at that aforementioned fluence was performed to simulate the conditions of Kr^{2+} irradiation encountered in space environments, and the resulting impact on the Au/Ni/nitrogen-doped 4H–SiC diodes was characterized using DLTS to study the behaviour, identify and quantify the various deep level defects that were induced by the swift heavy ion irradiation. Also, the role of annealing in restoring the non-rectifying diodes was reported. The findings from this research will offer a valuable understanding of the performance of Au/Ni/nitrogen-doped 4H–SiC Schottky barrier diodes when subjected to Kr^{2+} irradiation, potentially enhancing the radiation tolerance of devices fabricated for modern days electronic applications.

2 Experimental details

A nitrogen-doped 4H–SiC epitaxial layer with a doping concentration of approximately 4.0 × 10^{14} cm^{-3} (low doping density) sold by Cree Research Inc. was employed for this research. The epitaxial layer was grown by chemical vapour deposition on n^{+}–4H–SiC substrate with a doping concentration of 1.0 × 10^{18} cm^{-3}. The wafer supplied was polished on the two sides and had silicon-face epi ready with a resistivity of 0.02 Ω-cm. Small pieces of the samples with dimension ~ 2 mm × ~ 4 mm were cut from the large wafer (100.0 mm in diameter).

Before the ohmic contact was deposited on the higher doped side of the 4H–SiC, chemical degreasing was carried out by boiling in three organic solvents (trichloroethylene, acetone, and methanol) for 5 min each. The samples were thereafter rinsed in deionized water for approximately one minute before etching in 40% hydrofluoric acid for 30 s [9, 10]. Rinsing of the nitrogen-doped 4H–SiC samples in deionized water was carried out, followed by nitrogen gas blow drying. The grease and oxide layer on the substrates were removed by degreasing and etching, respectively [9, 22, 41, 42]. The effect of grease and the native oxide layer cannot be neglected because they affect the yield and reproducible process in the fabrication of microelectronic devices [43]. An ohmic contact of 3000 Å of nickel was subsequently thermally evaporated on the face with the higher doping concentration (1.0 × 10^{18} cm^{-3}) of the nitrogen-doped

4H–SiC at a deposition rate of approximately 1 Ås^{-1}. The vacuum pressure during the deposition was kept at ~ 5.2 × 10^{-6} mbar. The deposition rate and vacuum pressure, as well as the Ni evaporated thickness, were remotely monitored and recorded to get accurate thickness for ohmic and Schottky contacts. To lower the contact resistance, the fabricated Ni ohmic contact was transformed to Ni silicide by annealing at 950 °C for approximately 10 min in flowing argon in a quartz-tube furnace [44]. Annealed samples were left in the furnace to cool down to room temperature (300 K) before removing them.

After annealing the ohmic contact (i.e., before deposition of the SBDs) the sample was again cleaned in the three organic solvents as described before. This was done to remove any unnoticeable flake and dirt that was in contact with samples during the annealing and cooling, which might have a significant influence on the contact resistance. The Au/Ni (1:4) Schottky contacts of thickness and diameter 1000 Å (i.e., in the ratio of 1 to 4 for Au and Ni) and 0.6 mm, respectively, were resistively deposited at the moderate deposition rate of 0.4 Ås^{-1} in a vacuum pressure of ~ 2 × 10^{-6} mbar. The SBDs were deposited on the epilayer side with a lower doping concentration of approximately 4 × 10^{14} cm^{-3}. A schematic diagram of the nitrogen-doped 4H–SiC sample is shown in Fig. 1.

The electrical characterization of the SBDs at 300 K was carried out using a current–voltage (I–V) and capacitance–voltage (C–V) station comprising a pA-Meter/DC Voltage Source and an LF Impedance Analyzer, respectively. This characterization was done to determine the devices' quality purpose before proceeding to DLTS characterization. After the suitability of the devices was ascertained, the samples were mounted on a close-cycle helium cryostat to carry the DLTS measurements. The helium cryostat was closed to leave the device under vacuum and later pumped down to the desired measuring temperature before the characterization of the defect(s) present in the pristine device with the help of state-of-the-art DLTS. The DLTS measurements were performed using a Boonton 7200 capacitance meter. The signatures of the individual defect present were determined by DLTS.

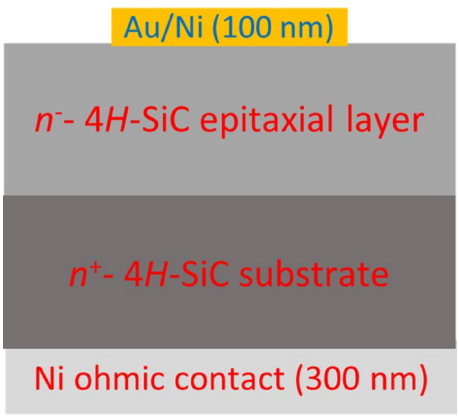

Fig. 1 Schematic diagram of 4H–SiC substrate after the thermally evaporation of Au/Ni Schottky contacts and a Ni ohmic contact. Nitrogen-doped 4H–SiC before and after isochronally annealing at 300 °C and 400 °C, measured at room temperature

Afterwards, the pristine Au/Ni/nitrogen-doped 4H–SiC SBDs were exposed to 107 MeV Kr^{2+} at a fluence of 1.0 × 10^{10} cm^{-2} in the IC-100 FLNR cyclotron radiation facility. The Stopping and Range of Ions in Matter (SRIM) 2010 code was employed to estimate the projected range and nuclear energy loss as well as the electronic energy loss of the Kr^{2+} irradiation [45]. Before the irradiation of pristine devices with Kr^{2+}, the expectation from the projected range, nuclear and electronic energy loss was 11.7 µm, 0.039 keV. nm^{-1} and 13.5 keV.nm^{-1}. The projected range of 11.7 µm expected is greater than the combined thickness of metal contact (0.10 µm) and that of epilayer (6.00 µm). Therefore, the swift ions (Kr^{2+}) are expected to go through both the diode and the epilayer and induce defects in the region of the bulk of the 4H-SiC sampled.

The swift heavy ion-irradiated devices were characterized using the I–V and C–V measuring system together with DLTS to compare the performance of the irradiated devices to that of pristine devices. The irradiated devices were thereafter annealed at 300 °C, and the same characterizations were repeated on the annealed samples.

3 Results and discussion

3.1 Current–voltage and capacitance–voltage characterization

To investigate the effect of swift iron (Kr^{2+}) irradiation on the I–V properties of the Au/Ni/nitrogen-doped 4H–SiC SBDs, the pristine devices were first characterized. A semi-logarithmic graph of the data obtained was plotted as shown in Fig. 2 (inverted solid triangles). It can be observed from the graph that

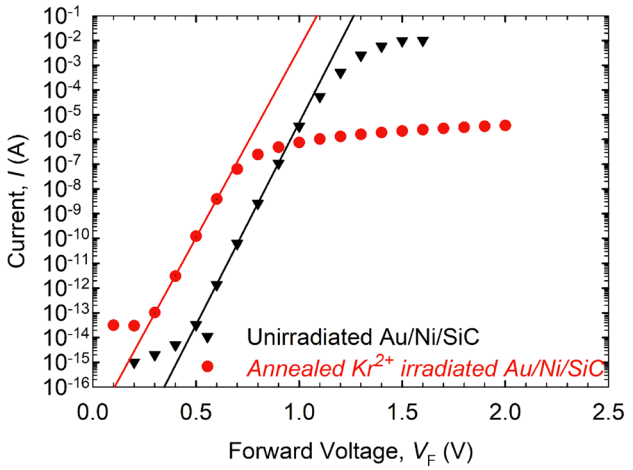

Fig. 2 Semi-log forward C–V characteristics of the Au/Ni/4H–SiC Schottky barrier diodes obtained before irradiation and after annealing the 107 MeV Kr^{2+} irradiated Au/Ni/4H–SiC Schottky barrier diodes at 300 °C. Measured at 300 K

I-V characteristics are linear on the semi-logarithmic scale at low bias up to 1.0 V (i.e. 3.4×10^{-14} A), which later deviated at high bias because of the influence of series resistance [46, 47]. The experimental data were fitted using conventional thermionic emission theory so as to evaluate some of the electrical parameters of the diodes [2, 48]. The values obtained are presented in Table 1. The ideality factor, n, was determined to be 1.04 from the gradient of the linear part of the semi-log plot, which was close to the ideal of unity. From the intercept of the log I-V plot, the Schottky barrier height for I-V ($SBH_{I\text{-}V}$) was determined to be 1.92 eV. The value of $SBH_{I\text{-}V}$ is high enough, though slightly less than the value of 2.5 eV predicted by the Schottky–Mott Model [49]. The series resistance, R_s, and the saturation current I_s, were determined to be 29 Ω and 2.3×10^{-22} A, respectively. From the ideality factor close to unity, the low series resistance and the low reverse leakage current, it can be deduced from the value obtained that the thermionic emission process is the dominant current transport mechanism in the pristine Au/Ni/4H-SiC diode. From the semi-logarithmic plot and the electrical parameters obtained for the pristine device, the device is of good quality and suitable for this research.

After the irradiation of the device with 107 MeV Kr^{2+} at a fluence of 1.0×10^{10} cm^{-2}, severe degradation was observed. The severe gradation was observed because of the low doping density of the sample used as well as the fluence at which the irradiation was carried out. The device turned to ohmic and lost all the rectification properties which was due to a very high series resistance. The exposure of the Au/Ni/nitrogen-doped 4H–SiC SBDs to Kr^{2+} has induced defects and caused changes/displacements at the interface of metal–semiconductor (i.e. Au/Ni–4H–SiC) which have altered the Schottky barrier height. The purpose of irradiating the diodes at that fluence was to determine if the annealing process could restore the rectification lost due to swift heavy ion, Kr^{2+} to measurable state, and bring about new defects associated with Kr^{2+}, which may likely be of significance in space applications. Before proceeding with characterization, the diode was annealed at 300 °C under the argon environment. Hereafter, partial rectification was observed (i.e., measurable state), as shown in Fig. 2 (solid circles). Partial rectification occurred because annealing at 300 °C provided sufficient thermal energy to allow the displaced atoms to become mobile and recombine with vacancies, effectively removing or rearranging the radiation-induced defects in 4H–SiC. The annealing process restored the crystalline structure of the devices and thereby improved their electrical properties. The plot was also linear at low forward biases up to 0.7 V (6.4×10^{-22} A) but deviated greatly at high biases which was due to series resistance because of high irradiation to low doping density devices. Forward current increases with an increase in bias up to 0.9 V. By comparing the two plots (unirradiated and

Table 1 Results of some electrical parameters calculated from I–V and C–V before irradiation and after annealing with 107 MeV Kr^{2+} irradiation of Au/Ni/4H–SiC SBD at 300 °C

Process	$n \pm 0.01$	R_S (Ω)	I_s (A)	N_d–N_a (cm^{-3})	V_{bi} (V)	$SBH_{I\text{-}V}$ (eV) ± 0.01	$SBH_{C\text{-}V}$ (eV) ± 0.01	C (pF) at − 5 V
Unirradiated	1.04	29	2.3×10^{-22}	5.9×10^{14}	1.64	1.53	1.92	8.66
After Kr^{2+} irradiation and annealing at 300 °C	1.11	327 k	2.5×10^{-18}	6.0×10^{14}	9.76	1.29	10.1	5.13

annealed after Kr^{2+} irradiation), it can be observed that in the region dominated by thermionic emission, the annealed after irradiation plot shifted upward (i.e., the forward current increased) and the maximum forward current was approximately 10^{-6} A. The parameters calculated from the graph are recorded in Table 1. The ideality factor increased to 1.11, the SBH decreased to 1.29 eV, and the series resistance increased greatly to 327 kΩ after annealing the irradiated device at 300 °C. The observation after irradiation indicates that another current transport mechanism apart from the thermionic emission process took place which might have resulted from defects introduced by Kr^{2+}.

Figure 3 shows the plots of capacitance versus bias voltage for the pristine and annealed at 300 °C after irradiation with Kr^{2+}. Before the irradiation, the plot with an inverted solid triangle was obtained. It could be observed from the plot that the capacitance decreased with increasing reverse bias voltage for pristine (before irradiation). After annealing the irradiated diode, the plot shows that the capacitance decreased significantly at zero bias and decreased at a lower rate under increasing reverse. From the plots, the capacitances at bias of − 5.0 V prior to irradiation and after annealing the irradiated diode were estimated from the plot to be 8.66 and 5.13 pF, respectively. The capacitance after irradiation decreased, which may be due to deep levels induced in the diode. The corresponding trend

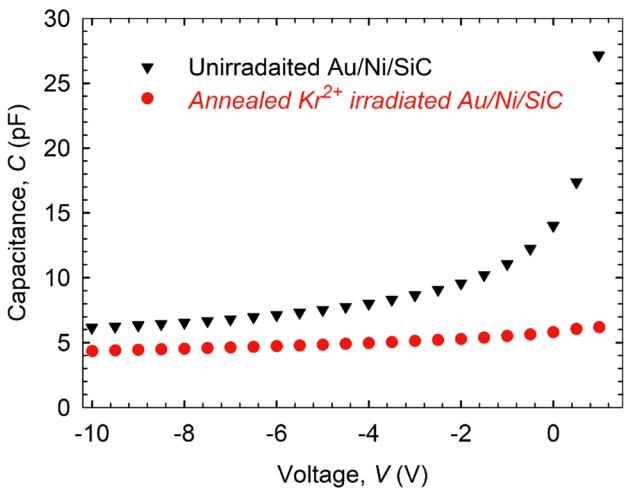

Fig. 3 Capacitance as a function of voltage characteristics of Schottky barrier diodes obtained before irradiation and after annealing the 107 MeV Kr^{2+} irradiated Au/Ni/4H–SiC Schottky barrier diode at 300 °C. Measured at 300 K

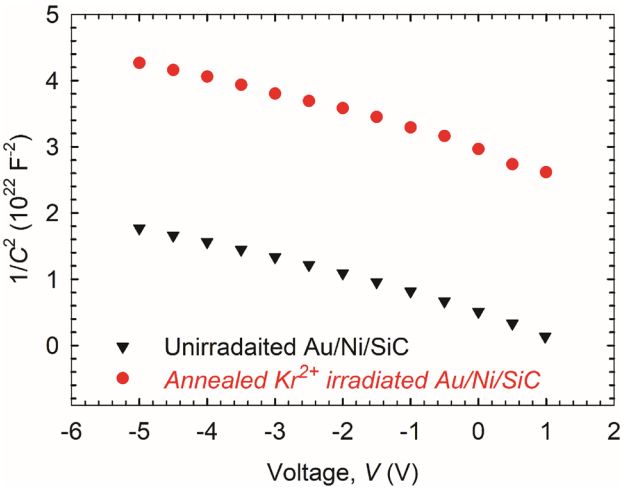

Fig. 4 $1/C^2$ as a function of voltage characteristics of Schottky barrier diodes obtained before irradiation and after annealing the 107 MeV Kr^{2+} irradiated Au/Ni/4H–SiC Schottky barrier diode at 300 °C. Measured at 300 K

is observed in the plot of C^{-2} versus bias voltage in pristine and after annealing the irradiated device, as depicted in Fig. 4. The linear part of the plots was fitted, and some parameters such as Schottky barrier height (C–V), built-in voltage (V_{bi}) and net doping carrier concentration (N_d–N_a) were determined and recorded in Table 1. It is observed from Table 1 that the value of SBH for the C–V (SBH_{CV}) is extremely high compared to that of the I-V (SBH_{IV}), which is as a result of the irradiation [9, 50]. Irradiation probably depleted all the carriers in the layer beneath the Schottky barrier diode, resulting in a region of effectively undoped material, possibly to the depth of the epilayer. This would add additional capacitance in series and lead to unrealistically high values of SBH for C–V. It is worth noting from Table 1 that the net carrier concentration after annealed the irradiated device increased to 6.0×10^{14} cm^{-3} compared to 5.9×10^{14} cm^{-3} before irradiation. It is well understood that irradiation induces deep level defects within the bandgap of a semiconductor (4H–SiC) which degrade the performance thereby reducing the carrier concentration. The increase in the net carrier concentration observed in this study may be as result of the introduction of shallow donor levels by irradiation which are close to the conduction band. These shallow levels can ionize easily at room temperature thereby contribute additional free carriers to the 4H–SiC. This unusual scenario may be as a

result of post-irradiation annealing on the devices which can sometimes activate additional dopants or repair some types of irradiation-induced damage, leading to an increase in carrier concentration.

Since the built voltage is directly proportional to the net concentration, an increase in the net carrier concentration led to an increase in built-in voltage.

3.2 DLTS characterization

DLTS characterization was carried out on the Au/Ni/4H-SiC SBDs to determine the *signature* of the defects present in the pristine as well as the defects induced after irradiation. The characterization took place from 22 to 360 K at a rate window of 2.5–1000 s^{-1}. From Fig. 5 (broken line), four deep level defects were observed in the pristine diode at measuring bias conditions of − 5.0 V with filling pulse amplitude and filling pulse amplitude of 6.0 V (i.e. 1.0–(− 5.0 V)) and 2.0 ms, respectively. Since the irradiated diode was not rectifying after being bombarded with Kr^{2+}, the DLTS characterization could not be carried out. The conditions for DLTS measurement to take place are as follows: the rectification of the SBD such as high SBH (greater than 1), n close to 1, leakage current and series resistance as well as the dissipation factor should be low [20]. The irradiated diode was thereafter annealed at 300 °C in an argon environment for partial recovery of the rectification. However, the series resistance was still very high. Based on the result obtained for electrical parameters in the previous section, the DLTS characterization can be carried out on the annealed irradiated diode. Figure 5 (unbroken line) depicts the DLTS spectrum of the irradiated Au/Ni/4H-SiC SBD after annealing at 300 °C under the same measuring conditions as that of the diode before irradiation. From the DLTS spectra obtained at rate window 2.5 –1000 s^{-1}, the activation energy below the conduction band minimum, E_T, and the apparent capture cross section, σn, were calculated from the Arrhenius plot as depicted in Fig. 6. Figure 6 shows the activation energies of four (4) defects (100, 120, 160 and 670 meV) observed before irradiation, as it was obtained from the gradient of the graph $\log\left[\frac{T^2}{e_n}\right](K^2s)$ as a function of $T^{-1}(K^{-1})$, (where T and e_n are temperature and emission rate, respectively), as well as the five (5) defects (100, 280, 410, 670 and 760 meV) obtained after annealing the Kr^{2+} irradiated diode [37]. The defects and their attributions are recorded in Table 2. As it has been reported earlier, the defect with an activation energy of 100 meV could be assigned to nitrogen impurity, which resides in the cubic site [51]. The intensity of the peak that stands for $E_{0.10}$ before irradiation is very prominent, unlike that obtained after annealing the Kr^{2+} irradiated device. The smaller peak obtained after annealing the Kr^{2+} irradiated device could be related to intense or heavy damage that lowers the position of the Fermi level deeper into the bandgap of 4H-SiC [52]. It could also be observed that the two deep level defects with activation energies of 120 and 160 meV,

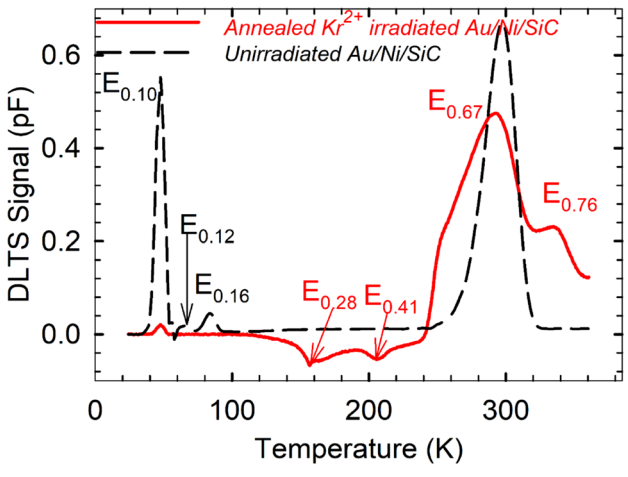

Fig. 5 DLTS spectra obtained before and after annealing the 107 MeV Kr^{2+} irradiated Au/Ni/4H–SiC Schottky barrier diode at 300 °C. DLTS signal for the solid line was scaled up by a factor of 4

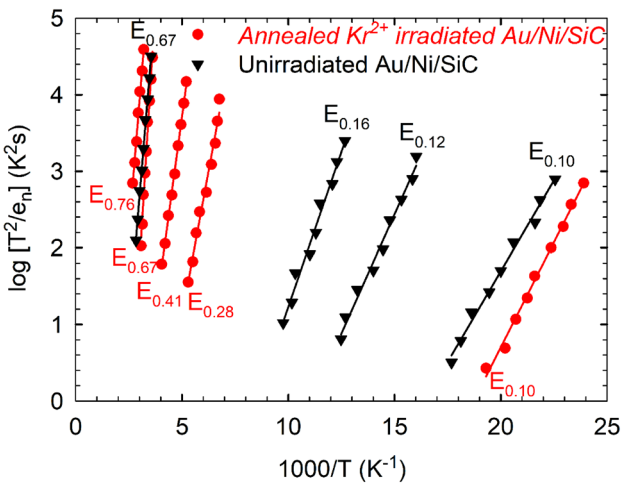

Fig. 6 Arrhenius plots of defects obtained before irradiation and after annealing the 107 MeV Kr^{2+} irradiated Au/Ni/4H–SiC Schottky barrier diode at 300 °C

Table 2 Deep level defects' *signatures* before irradiation and after annealing the 107 MeV Kr^{2+} irradiation of Au/Ni/4H-SiC SBD at 300 °C

Defect representation	E_C–E_T (meV)	σ_n (cm^2)	Defect attribution
$E_{0.10}$	100	5.5×10^{-12}	N [51]
$E_{0.12}$	120	??	Ti [53]
$E_{0.16}$	160	1.4×10^{-14}	Ti [54]
$E_{0.28}$	280	1.6×10^{-16}	I_C [25, 31]
$E_{0.41}$	410	5.7×10^{-15}	V_{Si} [25]
$E_{0.67}$	670	7.0×10^{-15}	V_C (Z_1/Z_2) [32]
$E_{0.76}$	760	1.2×10^{-14}	V_C (Z_1/Z_2) [32]

which have been attributed to titanium impurity, present in before irradiation were not detected or disappeared after irradiation with 107 MeV Kr^{2+} at fluence 1.0×10^{10} cm^{-2}. We could not ascertain that those two defects ($E_{0.12}$ and $E_{0.16}$) were not present, but the inability to observe them may be due to the intense damage to the devices. The intense damage to the device might have led to the position of Fermi level lowering deeper into the bandgap that might likely be below the shallow defect levels as it was observed with alpha-particle irradiated 4H-SiC at a fluence of 8.9×10^{11} cm^{-2} [52]. Two new defects (280 and 410 meV) with unusual behaviour, where the peaks were inverted and behaved like minority instead of majority carriers, were also observed. They were not observed in pristine diodes; therefore, they were related to Kr^{2+} irradiation. Defect $E_{0.28}$ (the activation energy of the defect) was not observed earlier, but it has an activation energy close to that of E0.32, which has been attributed to carbon interstitial [31]. The $E_{0.41}$ defect that was observed after Kr^{2+} irradiation has also been reported after exposing 4H–SiC to high-energy electrons and has been attributed to silicon vacancy [9]. It could be observed that the defects $E_{0.28}$ and $E_{0.41}$ behaved as minority carrier traps [40]. This unexpected behaviour of the device has been observed and reported for other semiconductor devices by Broniatowski et al. [40], which was associated to a very high series resistive material, where the DLTS signal is inverted when high series resistance was present. From Table 1, the value of series resistance obtained after irradiation was 327 kΩ and it can be concluded that high series resistance was responsible for the unexpected inverted DLTS peaks observed for the two new defects. The defect $E_{0.67}$ observed after Kr^{2+} irradiation was also observed to have the activation energy of 670 meV in pristine. Kr^{2+} irradiation also induced a defect with 760 meV, which has close activation energy with the defect induced by high-energy electron [9]. Both defects, $E_{0.67}$ and $E_{0.76}$, has been attributed to carbon vacancy which has been referred to as *Z1*/*Z2* defect [32].

4 Conclusions

Rectified Au/Ni/nitrogen-doped 4H–SiC SBDs have been fabricated using thermal evaporation techniques. The diodes were subjected to 107 MeV Kr^{2+} at the fluence of 1.0×10^{10} cm^{-2}. The effect of the irradiation at 1.0×10^{10} cm^{-2} fluence on diodes was observable from I–V and C–V leading to the loss of the SBDs' rectification properties. The series resistance of the diodes increased from 29 to MΩ after the irradiation. A degree of rectification was achieved after annealing the irradiated Au/Ni/nitrogen-doped 4H-SiC SBDs at a temperature of 300 °C, which made it possible to carry out DLTS measurements. Four defects were observed before irradiation while five defects were observed after annealing the Kr^{2+} irradiated SBD. Defects with activation energy of 100 meV's amplitude was reduced after irradiation, whereas the defects with energy 120 meV as well as 160 meV were not observed. It was concluded that the reduction in defect $E_{0.10}$ and disappearance of two defects ($E_{0.12}$ and $E_{0.16}$) could be attributed to the intense damage experienced by the device, which might have led to the position of Fermi level lowering deeper into the bandgap that might likely be below the shallow defect levels. The defects $E_{0.28}$ and $E_{0.41}$ were induced by Kr^{2+} irradiation and behaved weirdly in that it appeared as minority carriers and changed signs on the DLTS signal. The weird behaviour was related to the extreme value of series resistance with low capacitance.

Acknowledgements

This work is based on the research supported partly by the National Research Foundation (NRF) of South Africa. The authors acknowledged that opinions expressed, findings and conclusions arrived at are those of the authors and are not necessarily to be attributed to the NRF. The authors would like to

acknowledge Prof. Thulani Hlatshwayo for his assistance with the irradiation of the samples.

Author contributions

EO: Conceptualization, design of research, experimental, analysis, writing and reviewing the original draft. WEM: Review and edit of the original draft. EI: Review and edit the original draft.

Funding

Open access funding provided by University of Pretoria. The authors declare that no fund was received for this research.

Data availability

The datasets generated during and/or analysed during the current study are available from the author on reasonable request.

Declarations

Competing interest The authors declare that he has no known competing financial interests or personal relationships that could have appeared to influence the work reported in this paper.

References

1. B. Sharma, Metal-semiconductor Schottky barrier junctions and their applications, Springer Science & Business Media2013.
2. S.M. Sze, K.K. Ng, Physics of semiconductor devices, John Wiley & Sons2006.
3. M. Benlamri, B.D. Wiltshire, Y. Zhang, N. Mahdi, K. Shankar, D.W. Barlage, High breakdown strength Schottky diodes made from electrodeposited ZnO for power electronics applications. ACS Appl. Electron. Mater. **1**(1), 13–17 (2019)
4. I. Capan, 4H–SiC Schottky barrier diodes as radiation detectors: a review. Electronics **11**(4), 532 (2022)
5. J. Qi, X. Yang, X. Li, K. Tian, M. Wang, S. Guo, M. Yang, Temperature dependence of 1.2 kV 4H-SiC schottky barrier diode for wide temperature applications, 2019 IEEE 10th International Symposium on Power Electronics for Distributed Generation Systems (PEDG), IEEE, 2019, pp. 822-826
6. S.O. Tan, Comparison of graphene and zinc dopant materials for organic polymer interfacial layer between metal semiconductor structure. IEEE Trans. Electron Dev. **64**(12), 5121–5127 (2017)
7. G. Bellocchi, M. Vivona, C. Bongiorno, P. Badalà, A. Bassi, S. Rascuna, F. Roccaforte, Barrier height tuning in Ti/4H-SiC Schottky diodes. Solid-State Electron. **186**, 108042 (2021)
8. R. Yakimova, C. Hemmingsson, M. Macmillan, T. Yakimov, E. Janzén, Barrier height determination for n-type 4H-SiC schottky contacts made using various metals. J. Electron. Mater. **27**, 871–875 (1998)
9. E. Omotoso, W.E. Meyer, F.D. Auret, A.T. Paradzah, M. Diale, S.M.M. Coelho, P.J. Janse van Rensburg, The influence of high energy electron irradiation on the Schottky barrier height and the Richardson constant of Ni/4H-SiC Schottky diodes. Mater. Sci. Semicond. Process. **39**, 112–118 (2015)
10. A.T. Paradzah, E. Omotoso, M.J. Legodi, F.D. Auret, W.E. Meyer, M. Diale, Electrical characterization of high energy electron irradiated Ni/4H-SiC schottky barrier diodes. J. Electron. Mater. **45**(8), 4177–4182 (2016)
11. V. Gora, A. Chawanda, C. Nyamhere, F.D. Auret, F. Mazunga, T. Jaure, B. Chibaya, E. Omotoso, H.T. Danga, S.M. Tunhuma, Comparison of nickel, cobalt, palladium, and tungsten Schottky contacts on n-4H-silicon carbide. Phys. B **535**, 333–337 (2018)
12. Z. Zhou, W. He, Z. Zhang, J. Sun, A. Schöner, Z. Zheng, Characteristics of Ni-based ohmic contacts on n-type

4H-SiC using different annealing methods. Nanotechnol. Precision Eng. **4**(1), 013006 (2021)
13. S. Oh, G. Yang, J. Kim, Electrical characteristics of vertical Ni/β-Ga2O3 Schottky barrier diodes at high temperatures. ECS J. Solid State Sci. Technol. **6**(2), Q3022 (2016)
14. E. Omotoso, W.E. Meyer, E. Igumbor, T.T. Hlatshwayo, A.R. Prinsloo, F.D. Auret, C.J. Sheppard, DLTS study of the influence of annealing on deep level defects induced in xenon ions implanted n-type 4 H-SiC. J. Mater. Sci.: Mater. Electron. **33**(19), 15679–15688 (2022)
15. E. Omotoso, A. Paradzah, P.J. van Rensburg, M. Legodi, F. Auret, E. Igumbor, H. Danga, M. Diale, W. Meyer, Electrical characterisation of deep level defects created by bombarding the n-type 4H–SiC with 1.8 MeV protons. Surf. Coatings Technol **355**, 2–6 (2018)
16. R.R. Lamichhane, N. Ericsson, S. Frank, C. Britton, L. Marlino, A. Mantooth, M. Francis, P. Shepherd, M. Glover, S. Perez, A wide bandgap silicon carbide (SiC) gate driver for high-temperature and high-voltage applications, 2014 IEEE 26th International Symposium on Power Semiconductor Devices & IC's (ISPSD), IEEE, 2014, pp. 414-417
17. L. Lin, L. Zhu, R. Zhao, H. Tao, J. Huang, Y. Xu, Z. Zhang, First-principles study on ferromagnetism in 4H-SiC codoped with Al and Mn. New J. Chem. **42**(12), 9393–9397 (2018)
18. E. Igumbor, G. Dongho-Nguimdo, R.E. Mapasha, E. Omotoso, W.E. Meyer, Stability, electronic and defect levels induced by substitution of Al and P pair in 4H–SiC. J. Phys. Chem. Solids **142**, 109448 (2020)
19. R. Trew, Wide bandgap semiconductor transistors for microwave power amplifiers. IEEE Microwave Mag. **1**(1), 46–54 (2000)
20. E. Omotoso, Electrical characterization of process-and radiation-induced defects in 4H-SiC, University of Pretoria, 2015.
21. F. Roccaforte, P. Fiorenza, M. Vivona, G. Greco, F. Giannazzo, Selective doping in silicon carbide power devices. Materials **14**(14), 3923 (2021)
22. E. Omotoso, W.E. Meyer, F.D. Auret, A.T. Paradzah, M. Diale, S.M.M. Coelho, P.J. Janse van Rensburg, P.N.M. Ngoepe, Effects of 5.4 MeV alpha-particle irradiation on the electrical properties of nickel Schottky diodes on 4H–SiC. Nucl. Instrum. Methods Phys. Res. Sect. B: Beam Int. with Mater. Atoms **365**, 264–268 (2015)
23. J. Grant, W. Cunningham, A. Blue, V. O'Shea, J. Vaitkus, E. Gaubas, M. Rahman, Wide bandgap semiconductor detectors for harsh radiation environments. Nucl. Instrum. Methods Phys. Res., Sect. A **546**(1–2), 213–217 (2005)
24. C. Hemmingsson, N.T. Son, O. Kordina, J.P. Bergman, E. Janzén, J.L. Lindström, S. Savage, N. Nordell, Deep level defects in electron-irradiated 4H SiC epitaxial layers. J. Appl. Phys. **81**(9), 6155–6159 (1997)
25. J. Doyle, M.K. Linnarsson, P. Pellegrino, N. Keskitalo, B. Svensson, A. Schoner, N. Nordell, J. Lindstrom, Electrically active point defects in n-type 4H–SiC. J. Appl. Phys. **84**(3), 1354–1357 (1998)
26. E. Viswanathan, R. Murugaraj, S. Sankar, A. Arulchakkaravarthi, D. Kanjilal, K. Sivaji, Low temperature dielectric study on swift heavy ion irradiated 6H-SiC crystals. Trans. Indian Inst. Met. **64**(3), 305–308 (2011)
27. E. Kalinina, G. Onushkin, D. Davidov, A. Hallen, A. Konstantinov, V. Skuratov, J. Stano, Electrical study of 4H-SiC irradiated with swift heavy ions, 12th International Conference on Semiconducting and Insulating Materials, 2002. SIMC-XII-2002., IEEE, 2002, pp. 106–109.
28. S. Wei, Z. Yin, J. Bai, W. Xie, F. Qin, Y. Su, D. Wang, The structural and electronic properties of Carbon-related point defects on 4H–SiC (0001) surface. Appl. Surf. Sci. **582**, 152461 (2022)
29. H. Tsuchida, M. Ito, I. Kamata, M. Nagano, Formation of extended defects in 4H–SiC epitaxial growth and development of a fast growth technique. Phys. Status Solidi (b) **246**(7), 1553–1568 (2009)
30. X. Yan, P. Li, L. Kang, S.-H. Wei, B. Huang, First-principles study of electronic and diffusion properties of intrinsic defects in 4H–SiC. J. Appl. Phys. **127**(8), 085702 (2020)
31. A. Castaldini, A. Cavallini, L. Rigutti, F. Nava, Low temperature annealing of electron irradiation induced defects in 4 H-SiC. Appl. Phys. Lett. **85**(17), 3780–3782 (2004)
32. N.T. Son, X.T. Trinh, L.S. Løvlie, B.G. Svensson, K. Kawahara, J. Suda, T. Kimoto, T. Umeda, J. Isoya, T. Makino, T. Ohshima, E. Janzén, Negative-U system of carbon vacancy in 4H–SiC. Phys. Rev. Lett. **109**(18), 187603 (2012)
33. E. Chong, B.-H. Park, H.-Y. Cha, K. Choi, D.-H. Lee, Analysis of defect-related electrical fatigue in 4H–SiC avalanche photodiodes. IEEE Photonics Technol. Lett. **30**(10), 899–902 (2018)
34. S. Xiao, S. Harada, K. Murayama, T. Ujihara, Characterization of V-shaped defects formed during the 4H-SiC solution growth by transmission electron microscopy and X-ray topography analysis. Cryst. Growth Des. **16**(9), 5136–5140 (2016)
35. S.M. Tunhuma, M. Diale, J.M. Nel, M. Madito, T.T. Hlatshwayo, F.D. Auret, Defects in swift heavy ion irradiated n–4H–SiC. Nucl. Instrum. Methods Phys. Res., Sect. B **460**, 119–124 (2019)
36. H. Jacobson, J. Birch, R. Yakimova, M. Syväjärvi, J. Bergman, A. Ellison, T. Tuomi, E. Janzén, Dislocation evolution in 4H–SiC epitaxial layers. J. Appl. Phys. **91**(10), 6354–6360 (2002)

37. F.D. Auret, P.N. Deenapanray, Deep level transient spectroscopy of defects in high-energy light-particle irradiated Si. Crit. Rev. Solid State Mater. Sci. **29**(1), 1–44 (2004)
38. E. Kalinina, G. Kholuyanov, G. Onushkin, D. Davydov, A. Strel'chuk, A. Konstantinov, A. Hallén, A.Y. Nikiforov, V. Skuratov, K. Havancsak, Optical and electrical properties of 4H–SiC irradiated with fast neutrons and high-energy heavy ions. Semiconductors **38**, 1187–1191 (2004)
39. E.V. Kalinina, G. Kholuyanov, G. Onushkin, D. Davydov, A.M. Strel'chuk, A. Zubrilov, A. Hallén, A.O. Konstantinov, V. Skuratov, J. Staňo, Electrical and optical study of 4H–SiC CVD epitaxial layers irradiated with swift heavy ions. Mater. Sci. Forum Trans. Tech. Publ. **433–436**, 467–470 (2003)
40. A. Broniatowski, A. Blosse, P. Srivastava, J. Bourgoin, Transient capacitance measurements on resistive samples. J. Appl. Phys. **54**(6), 2907–2910 (1983)
41. E. Omotoso, W.E. Meyer, F.D. Auret, M. Diale, P.N.M. Ngoepe, Response of Ni/4H-SiC Schottky barrier diodes to alpha-particle irradiation at different fluences. Phys. B **480**, 196–200 (2016)
42. A.T. Paradzah, F.D. Auret, M.J. Legodi, E. Omotoso, M. Diale, Electrical characterization of 5.4 MeV alpha-particle irradiated 4H-SiC with low doping density. Nucl. Instrum. Methods Phys. Res. Sect. B: Beam Int. Mater. Atoms **358**, 112–116 (2015)
43. R.E. Williams, Gallium arsenide processing techniques, Artech House1984.
44. T. Marinova, A. Kakanakova-Georgieva, V. Krastev, R. Kakanakov, M. Neshev, L. Kassamakova, O. Noblanc, C. Arnodo, S. Cassette, C. Brylinski, B. Pecz, G. Radnoczi, G. Vincze, Nickel based ohmic contacts on SiC. Mater. Sci. Eng., B **46**(1–3), 223–226 (1997)
45. J.F. Ziegler, M.D. Ziegler, J.P. Biersack, SRIM – The stopping and range of ions in matter (2010). Nucl. Instrum. Methods Phys. Res., Sect. B **268**(11), 1818–1823 (2010)
46. S.S. Naik, V.R. Reddy, Temperature dependency and current transport mechanisms of Pd/V/n-type InP schottky rectifiers. Adv. Mater. Lett. **3**(3), 188–196 (2012)
47. E. Omotoso, W.E. Meyer, S.M. Coelho, M. Diale, P.N.M. Ngoepe, F.D. Auret, Electrical characterization of defects introduced during electron beam deposition of W Schottky contacts on n-type 4H-SiC. Mater. Sci. Semicond. Process. **51**, 20–24 (2016)
48. E. Rhoderick, R. Williams, Metal-Semiconductor Contacts (2nd edn.) Clarendon, Oxford Science, Oxford, 1988
49. S.U. Omar, T.S. Sudarshan, T.A. Rana, H. Song, M. Chandrashekhar, Large barrier, highly uniform and reproducible Ni-Si/4H-SiC forward Schottky diode characteristics: testing the limits of Tung's model. J. Phys. D Appl. Phys. **47**(29), 295102 (2014)
50. F. Yakuphanoglu, B.F. Şenkal, Electronic and thermoelectric properties of polyaniline organic semiconductor and electrical characterization of Al/PANI MIS diode. J. Phys. Chem. C **111**(4), 1840–1846 (2007)
51. T. Kimoto, A. Itoh, H. Matsunami, S. Sridhara, L. Clemen, R. Devaty, W. Choyke, T. Dalibor, C. Peppermüller, G. Pensl, Nitrogen donors and deep levels in high-quality 4H–SiC epilayers grown by chemical vapor deposition. Appl. Phys. Lett. **67**(19), 2833–2835 (1995)
52. E. Omotoso, W.E. Meyer, F.D. Auret, A.T. Paradzah, M.J. Legodi, Electrical characterization of deep levels created by bombarding nitrogen-doped 4H-SiC with alpha-particle irradiation. Nucl. Instrum. Methods Phys. Res., Sect. B **371**, 312–316 (2016)
53. A.A. Lebedev, Deep level centers in silicon carbide: A review. Semiconductors **33**(2), 107–130 (1999)
54. T. Dalibor, G. Pensl, H. Matsunami, T. Kimoto, W. Choyke, A. Schöner, N. Nordell, Deep defect centers in silicon carbide monitored with deep level transient spectroscopy. Phys. Status Solidi (a) **162**(1), 199–225 (1997)